

Adapter Shield: A Unified Framework with Built-in Authentication for Preventing Unauthorized Zero-Shot Image-to-Image Generation

Jun Jia¹ Hongyi Miao² Yingjie Zhou¹ Wangqiu Zhou³ Jianbo Zhang¹ Linhan Cao¹
Dandan Zhu⁴ Hua Yang¹ Xionguo Min¹ Wei Sun⁴ Guangtao Zhai¹

¹Shanghai Jiao Tong University ²Shandong University

³Hefei University of Technology ⁴East China Normal University

jiajun0302@sjtu.edu.cn

Abstract

With the rapid progress in diffusion models, image synthesis has advanced to the stage of zero-shot image-to-image generation, where high-fidelity replication of facial identities or artistic styles can be achieved using just one portrait or artwork, without modifying any model weights. Although these techniques significantly enhance creative possibilities, they also pose substantial risks related to intellectual property violations, including unauthorized identity cloning and stylistic imitation. To counter such threats, this work presents **Adapter Shield**, the first **universal** and **authentication-integrated** solution aimed at defending personal images from misuse in zero-shot generation scenarios. We first investigate how current zero-shot methods employ image encoders to extract embeddings from input images, which are subsequently fed into the UNet of diffusion models through cross-attention layers. Inspired by this mechanism, we construct a reversible encryption system that maps original embeddings into distinct encrypted representations according to different secret keys. The authorized users can restore the authentic embeddings via a decryption module and the correct key, enabling normal usage for authorized generation tasks. For protection purposes, we design a multi-target adversarial perturbation method that actively shifts the original embeddings toward designated encrypted patterns. Consequently, protected images are embedded with a defensive layer that ensures unauthorized users can only produce distorted or encrypted outputs. Extensive evaluations demonstrate that our method surpasses existing state-of-the-art defenses in blocking unauthorized zero-shot image synthesis, while supporting flexible and secure access control for verified users.

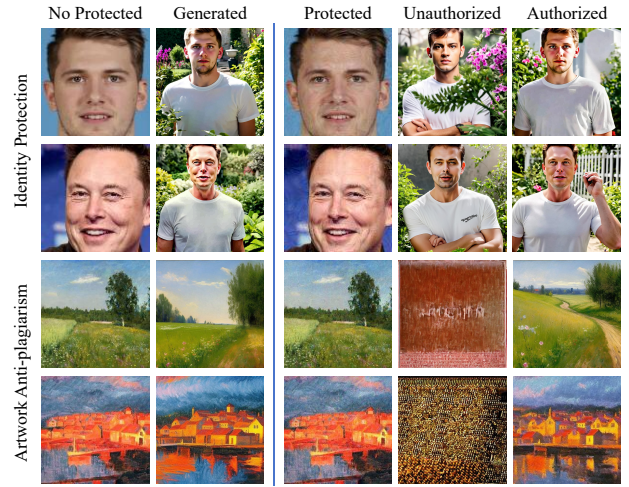


Figure 1. When publishing the original image without protection, diffusion models can easily imitate the content via just one image (**the second column**). After applying Adapter Shield (**the third column**), unauthorized users cannot generate the target content (**the fourth column**) while authorized users can generate intended images through a password-based authentication (**the fifth column**).

1. Introduction

With the development of diffusion models, image generation has evolved from early text-to-image methods [14] to the current framework that supports multimodal conditional inputs, in which text and visual inputs jointly guide the generation process. Recently, many zero-shot image-to-image generation approaches are proposed, which can synthesize highly similar facial identities or artistic styles with only a single portrait or artwork as input. Unlike fine-tuning diffusion models, these approaches do not alter the pre-trained parameters of diffusion models. Instead, they inject the key information of reference images into diffusion models in a plug-and-play manner, thereby offering substantial conve-

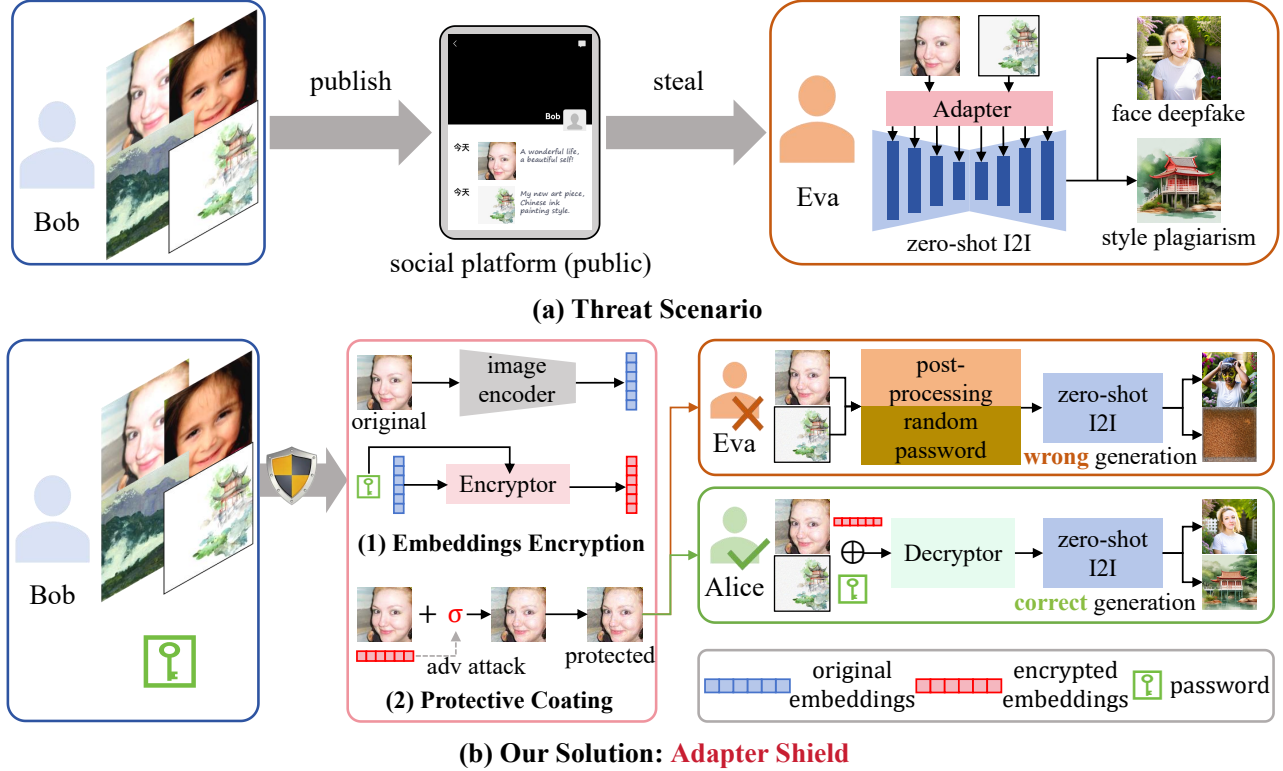


Figure 2. (a) the threat scenario of this paper: personal images can be imitated by zero-shot image-to-image generation based on diffusion models. (b) the proposed solution (the red box): adding a protective coating to the original images, ensuring **universal** and **authentication-integrated**.

nience to AI-generated content (AIGC) creators. However, despite their widespread adoption, these technologies have also introduced security risks associated with image contents. The primary concern lies in copyright infringement: unauthorized synthesis of facial identity and artistic style may violate individuals' rights to their portrait and artists' intellectual property rights. Moreover, the generation of sensitive or harmful content using personal portraits could lead to adverse societal consequences. For this concern, although deepfake detection technology has made significant progress, it remains reactive, addressing problems only after they occur. Therefore, to protect personal images from unauthorized zero-shot image-to-image generation, there is an urgent need to develop a proactive protection mechanism that establishes AIGC usage permissions at the source of image generation.

Compared to fine-tuning diffusion models, the zero-shot image-to-image generation approaches treat images in a similar way as text prompts. These approaches use an image encoder to extract image embeddings and incorporate an additional cross-attention module that decouples the embeddings of text and image prompts. In practical scenarios, such methods can replicate the target facial identity or artistic style using only a single image as reference. Compared

to fine-tuning-based approaches, these zero-shot methods present a more significant risk, as unauthorized users can achieve their goals with just one image, which is considerably easier to obtain than the larger dataset required for fine-tuning. Therefore, preventing unauthorized generation with zero-shot image-to-image methods requires increased attention, as no universal and flexible solution has yet been developed to address this challenge. Recently, Song *et al.* [19] propose IDProtector, a data poisoning-based method tailored to facial identity protection. However, IDProtector has two significant limitations: (1) this method is irreversible, and even trusted parties cannot recover the true identity, thereby limiting its flexibility; (2) it focuses exclusively on unauthorized identity forgery while overlooking the other critical issue in real scenarios: style plagiarism of artworks.

To safeguard personal images from being forged or plagiarized by unauthorized zero-shot image-to-image generation methods, this paper begins by systematically analyzing the major challenges in this scenario. There are two primary challenges which remain insufficiently addressed: **(1) Universality:** The protection solution should be effective across various zero-shot image-to-image methods and diverse threat scenarios such as identity forgery and artistic style plagiarism. **(2) Authentication:** The image owner

holds the authority to define permitted usage scenarios. While image post-processing operations can remove added protection information from protected images, unauthorized users may also exploit this technique. Therefore, the protection solution must exhibit robustness against common post-processing techniques while permitting authorized users to produce intended outputs securely.

To address these challenges, this paper proposes **Adapter Shield**, the first **universal** and **authentication-integrated** framework against unauthorized zero-shot image-to-image generation. As shown in Fig. 2, the framework first encrypts the original image embeddings required by zero-shot image-to-image generation methods. Then, a protective coating related to the encrypted embeddings are added to the original image through the proposed multi-targeted adversarial attack. Consequently, unauthorized users cannot replicate the original content based on the protected image, while authorized users can recover the original embeddings for intended generation using the correct decryption password. The protection results are shown in Figure 1. The main contributions of this work include:

- We propose the first **universal** and **authentication-integrated** framework for preventing unauthorized zero-shot image-to-image generation.
- The proposed framework provides flexible access control through password-based authentication, allowing different passwords to generate diverse protected images.
- The proposed framework shows superior universality across various tasks and diverse fine-tuning methods.

2. Related Work

2.1. Zero-shot I2I Generation based on Diffusion

Fine-tuning technologies for diffusion models, which involve optimizing all or part of the model parameters using a small-scale dataset, enable the generation of content that closely resembles the images used during fine-tuning. However, these methods still require multiple images representing a specific character or style, such as LoRA [6], DreamBooth [15], Textual Inversion [3], and Custom Diffusion [8]. Nevertheless, acquiring such multiple images is often challenging in practice. To address this, zero-shot image-to-image generation methods have been developed, requiring only a single image to produce similar content. These methods use an image encoder to extract embeddings from the single reference image and a cross-attention module to integrate them into specific UNet layers. For general generation, IP-Adapter [24] employs CLIP [13] as the image encoder. For facial identity generation, IP-Adapter Faceid [24] and Instant-ID [22] encode embeddings through pretrained ArcFace [2] models. Recent methods such as Photomakerr [10], PULID [5], and StoryMaker [27] further integrate both CLIP and ArcFace encoders to enhance iden-

tity preservation. Compared to fine-tuning, these zero-shot methods alleviate the necessity of acquiring multiple fine-tuning images, thereby enhancing their practical applicability.

2.1.1. Image Protection for Diffusion Models

The growing use of fine-tuning technologies in diffusion models has raised increasing concerns about the unauthorized use of personal images. To address this risk, numerous methods have been proposed to protect copyrighted content, such as artistic styles [17] and facial identities [21], from being reproduced by fine-tuning. Adv-DM (mist) [11] targets the fine-tuning of diffusion models to output a predefined noisy image by adding pixel-level adversarial perturbations to original images. CAAT [23] demonstrates that subtle perturbations in the attention mechanism can induce strong fine-tuning misdirection. Pretender [20] proposes an adversarial training framework to effectively mislead downstream fine-tuning processes, demonstrating universality across various fine-tuning methods. ACE [26] introduce a unified target to guide perturbation optimization consistently across both the forward encoding and reverse generation processes, effectively addressing the off-set problem in this field and enhancing protection stability and transferability. Nightshade [18] implements a prompt-specific poisoning approach to mislead text-to-image models to generate incorrect results. For anti-plagiarism of artistic style, Glaze [17] proposes an optimization-based cloaking algorithm to obstruct the learning and replication of artistic style by diffusion models. For defending specific fine-tuning methods, Anti-DreamBooth [21] embeds imperceptible noise into training images to prevent fine-tuning by DreamBooth. In preventing zero-shot image-to-image generation, IDProtector [19] introduces a unified model that adds adversarial perturbations to disrupt the image encoders used by such methods.

3. Methodology

3.1. Threat Scenario

This section presents the real-world threat scenario faced by sharing personal images. We define three key parties involved: (1) **Bob**, (2) **Alice**, and (3) **Eva**. The specific objectives of each party are outlined as follows:

- **Bob**: as shown in Figure 2, Bob is the images' owner who hopes to publicly share his personal portraits or paintings. For the authorized party Alice, Bob permits the use of zero-shot image-to-image generative models to create derivative works from his images. In contrast, the unauthorized party Eva is prohibited from using such models to replicate his images.
- **Alice**: the authorized party with rights to use Bob's images. Given the correct password, Alice can recover the original image embeddings, enabling normal usage.

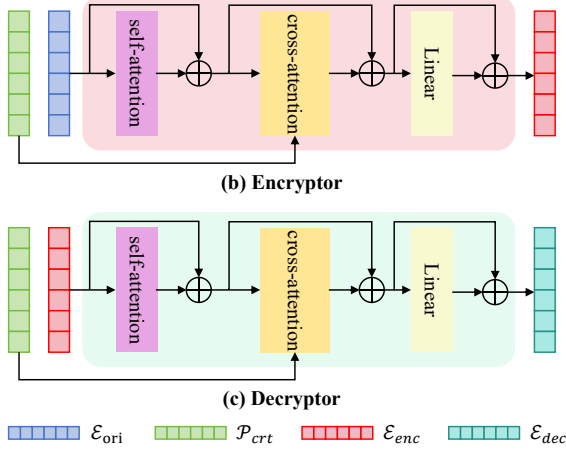


Figure 3. The details of the encryptor and decryptor. We omit layer normalization operation here.

- **Eva:** the unauthorized adversary attempting illicit usage. As shown in Figure 2 (b), Eva may try to remove the protection solution by applying post-processing operations to Bob’s images. Furthermore, in a more dangerous scenario, Eva obtains the decryption tool and attempts to guess the password to recover the original embeddings.

3.2. Pipeline of Adapter Shield

Based on the above analysis, existing zero-shot image-to-image generation methods generally employ an image encoder to extract image embeddings, and incorporate an additional cross-attention module to decouple the projected image embeddings from the text prompt embeddings. Therefore, the core idea of our solution is to disrupt the original embeddings of images, making them deviate from the initial form. To achieve this objective, Adapter Shield consists of two sequential stages: **(1) embeddings encryption** and **(2) protective coating generation**. We define the image encoder as **IE**, the diffusion model as **DM**, the proposed encryptor as **Enc**, the password as \mathcal{P}_{crt} , the original image as \mathcal{I}_{ori} , and the image embeddings as \mathcal{E} . The password and the embeddings to be encrypted have the same dimension.

3.2.1. Stage-1: Embeddings Encryption

Overall Pipeline: The image encoder **IE** is first used to extract original image embeddings \mathcal{E}_{ori} . Subsequently, \mathcal{E}_{ori} are encrypted into \mathcal{E}_{enc} by encryptor **Enc**, with the requirement that the similarity between \mathcal{E}_{enc} and \mathcal{E}_{ori} be as low as possible. This process can be formulated as:

$$\mathcal{E}_{enc} = \text{Enc}(\mathcal{E}_{ori}, \mathcal{P}_{crt}), \quad (1)$$

where $\mathcal{E}_{ori} = \text{IE}(\mathcal{I}_{ori})$. For the authorized user Alice, the encrypted embeddings \mathcal{E}_{enc} can be decrypted into \mathcal{E}_{dec} using the decryptor **Dec** and the correct password \mathcal{P}_{crt} .

This process achieves **authentication** for authorized users, which can be formulated as:

$$\mathcal{E}_{dec} = \text{Dec}(\mathcal{E}_{enc}, \mathcal{P}_{crt}). \quad (2)$$

Architecture of Encryptor and Decryptor: As illustrated in Figure 3, both the encryptor **Enc** and decryptor **Dec** are trainable models sharing the same architecture but differ in their parameters. The proposed encryptor and decryptor are composed of a self-attention module, a cross-attention module, and a fully connected layer. The cross-attention module enables the encrypted results to be dependent on the corresponding passwords.

Optimization Objectives: The primary optimization objectives involve minimizing the similarity between encrypted embeddings \mathcal{E}_{enc} and original embeddings \mathcal{E}_{ori} , while simultaneously maximizing the similarity between decrypted embeddings \mathcal{E}_{dec} and the original embeddings \mathcal{E}_{ori} . To achieve these objectives, we propose an encryption loss \mathcal{L}_{enc} and a decryption loss \mathcal{L}_{dec} based on cosine similarity **CosSim** inspired by facial de-identification [1, 4, 9], which guide the joint training of the encryptor and decryptor. When training, we randomly generate $n+1$ passwords that includes one correct password \mathcal{P}_{crt} and n wrong password \mathcal{P}_{wrg_i} , $i=\{0, 1, \dots, n-1\}$. The loss functions are formulated as follows:

$$\mathcal{L}_{enc} = \text{CosSim}(\text{Enc}(\mathcal{E}_{ori}, \mathcal{P}_{crt}), \mathcal{E}_{ori}) + \sum_{i=0}^{n-1} \text{CosSim}(\text{Enc}(\mathcal{E}_{ori}, \mathcal{P}_{wrg_i}), \mathcal{E}_{ori}), \quad (3)$$

$$\mathcal{L}_{dec} = 1 - \text{CosSim}(\text{Dec}(\mathcal{E}_{enc_crt}, \mathcal{P}_{crt}), \mathcal{E}_{ori}), \quad (4)$$

where $\mathcal{E}_{enc_crt} = \text{Enc}(\mathcal{E}_{ori}, \mathcal{P}_{crt})$. The range of cosine similarity is restricted between 0 and 1 to ensure the non-negativity. Furthermore, to prevent unauthorized users from recovering the original embeddings using random passwords, we propose \mathcal{L}_{wrg} as follows:

$$\mathcal{L}_{wrg} = \sum_{i=0}^{n-1} \text{CosSim}(\text{Dec}(\mathcal{E}_{enc_crt}, \mathcal{P}_{wrg_i}), \mathcal{E}_{ori}). \quad (5)$$

To enhance the diversity of encryption and decryption results, we propose \mathcal{L}_{div} . For each iterative optimization, the batch size is b . Thus, there are a total of $n+1$ encrypted embeddings and n wrong decrypted embeddings in each iteration. We re-number the above $b \times (2n+1)$ embeddings as from 0 to N , where $N=b \times (2n+1)-1$. \mathcal{L}_{div} is formulated as follows:

$$\mathcal{L}_{div} = \frac{1}{2} \sum_{k=0}^N \sum_{j=0}^N \text{CosSim}(\mathcal{E}_k, \mathcal{E}_j), \text{ s.t. } k \neq j. \quad (6)$$

This loss function enforces diverse encryption and decryption results when different passwords are applied, while

ensuring that distinct original embeddings do not generate similar encrypted or decrypted results with different passwords.

Finally, to prevent similarity in encryption and decryption results when the same password is applied to different original embeddings, we introduce $\mathcal{L}_{div.s}$. Specifically, in each iteration, for each original embedding in the same batch, two fixed passwords, \mathcal{P}_{enc} and \mathcal{P}_{dec} , are respectively used for encryption and decryption. $\mathcal{L}_{div.s}$ is formulated as follows:

$$\begin{aligned} \mathcal{L}_{div.s} = & \frac{1}{2} \sum_{k=0}^{b-1} \sum_{j=0}^{b-1} \text{CosSim}(\mathcal{E}_{enc,k}, \mathcal{E}_{enc,j}) + \\ & \frac{1}{2} \sum_{k=0}^{b-1} \sum_{j=0}^{b-1} \text{CosSim}(\mathcal{E}_{dec,k}, \mathcal{E}_{dec,j}) \text{ s.t. } k \neq j, \end{aligned} \quad (7)$$

where \mathcal{E}_{enc} and \mathcal{E}_{dec} represent the encrypted embeddings with \mathcal{P}_{enc} and the decrypted embeddings with \mathcal{P}_{dec} , respectively. In conclusion, the total loss function is the sum of the above-mentioned loss functions weighted by λ_i :

$$\mathcal{L} = \lambda_1 \mathcal{L}_{enc} + \lambda_2 \mathcal{L}_{dec} + \lambda_3 \mathcal{L}_{wrg} + \lambda_4 \mathcal{L}_{div} + \lambda_5 \mathcal{L}_{div.s}. \quad (8)$$

3.2.2. Stage-2: Protective Coating Generation

Overall Objectives: In the second stage, we generate a protective coating on the original image \mathcal{I}_{ori} by optimizing imperceptible perturbations δ . The adversarial perturbation budget is denoted by ϵ . The generation process of protected image \mathcal{I}_{pro} can be formulated as:

$$\begin{aligned} \mathcal{I}_{pro} = & \mathcal{I}_{ori} + \delta \\ \text{s.t. } & \max(\text{CosSim}(\mathbf{IE}_i(\mathcal{I}_{pro}), \mathcal{E}_{tar,i})) \\ & \text{and } |\delta| \leq \epsilon, i = \{0, 1, \dots, m-1\}, \end{aligned} \quad (9)$$

where $\mathcal{E}_{tar,i}$ denotes the encrypted embedding associated with the image encoder employed by the i^{th} zero-shot image-to-image method. There are a total of m encoders.

Robust Multi-targeted Adversarial Attack: As shown in Eq. 9, the objective of protective coating generation is to modify the original image embeddings \mathcal{E}_{ori} to the encrypted embeddings $\mathcal{E}_{tar,i}$ without significantly altering the original image quality. This process faces two primary challenges: (1) unauthorized adversaries may employ more than one zero-shot image-to-image generation methods, necessitating that the protective coating exhibits universality across various image encoders utilized in these methods; (2) unauthorized adversaries may attempt to erase the protective coating through image processing operations, such as blurring and noise addition. To effectively tackle these challenges, this paper proposes a robust multi-targeted adversarial attack method based on Fast Gradient Sign Method (FGSM).

To achieve **universality**, we design a multi-targeted adversarial loss function \mathcal{L}_{mt} as follows:

$$\mathcal{L}_{mt} = \sum_{i=0}^{m-1} 1 - \text{CosSim}(\mathcal{E}_{pro,i}, \mathcal{E}_{tar,i}), \quad (10)$$

where $\mathcal{E}_{tar,i} = \text{Enc}_i(\mathbf{IE}_i(\mathcal{I}_{ori}), \mathcal{P})$ and $\mathcal{E}_{pro,i} = \mathbf{IE}_i(\mathcal{I}_{pro})$. Then, the perturbations δ are updated by the gradients ∇ of \mathcal{I}_{ori} :

$$\delta = \delta - \sigma * \nabla_{\mathcal{I}_{adv}} \mathcal{L}_{mt}. \quad (11)$$

The range of δ is restricted between $-\epsilon$ and $+\epsilon$. To enhance robustness, we add differentiable image processing operations **diff_distortion** in each iteration. The above procedure is repeated until the similarity surpasses the predefined threshold *ths*. This algorithm is detailed in Algorithm 1.

Algorithm 1 Robust Multi-targeted Adversarial Attack

Input: $\mathcal{I}_{ori}, \mathcal{E}_{tar,i}, i = \{0, 1, \dots, m-1\}$

Output: \mathcal{I}_{pro}

```

1:  $\delta = 0, iter = 0, \mathcal{I}_{pro} = \mathcal{I}_{ori}$ 
2: while  $\text{CosSim}(\mathcal{E}_{pro,i}, \mathcal{E}_{tar,i}) > ths$  do
3:    $\mathcal{I}_{pro} = \mathcal{I}_{ori} + \delta$ 
4:    $\mathcal{I}_{pro} = \text{diff\_distortion}(\mathcal{I}_{pro})$ 
5:   for  $i \in [0, m-1]$  do
6:      $\mathcal{E}_{pro,i} = \mathbf{IE}_i(\mathcal{I}_{pro})$ 
7:   end for
8:    $\mathcal{L}_{mt} = \sum_{i=0}^{m-1} 1 - \text{CosSim}(\mathcal{E}_{pro,i}, \mathcal{E}_{tar,i})$ 
9:    $\delta = \delta - \sigma * \nabla_{\mathcal{I}_{adv}} \mathcal{L}_{mt}$ 
10:   $\delta = \text{clip}(\delta, \min=-\epsilon, \max=+\epsilon)$ 
11: end while
12: return Outputs

```

4. Experiments

4.1. Experimental Settings

Dataset: We evaluate the proposed approach on two typical tasks: facial identity protection and artwork anti-plagiarism. For facial identity protection, we use CelebA [12] for training and 200 facial images from FFHQ [7] for testing. All images are normalized to 112×112 by face alignment. For artwork anti-plagiarism, we select 25,769 painting images from Wikiart [16] as the training dataset and 50 painting images unseen in the training phase for test.

Implementation Details: In experiments, we select two distinct zero-shot image-to-image generation methods for each task ($m=2$ in Eq. 9). In the case of facial identity protection, IP-Adapter FaceID [24] based on SD-1.5 and Instant-ID [22] based on SDXL are selected. These methods use the same image encoder (ArcFace [2]) but differ in terms of their pre-trained models. For artwork

Table 1. Comparison results of facial identity protection and artwork anti-plagiarism tasks against SOTA methods. ISM: identity similarity between generated and original faces, AFR: abnormal face rate, ESM: embedding similarity between protected and original artworks. “specific” refers to the consideration of only a single type of image encoder, whereas “general” considers all types of image encoders. The best and second-best results are marked by red and blue.

Method	Face Identity Protection						Artwork Anti-Plagiarism					
	IP-Adapter Faceid			Instant-ID			IP-Adapter			IP-Adapter Plus		
	ISM↓	AFR↑	PSNR↑	ISM↓	AFR↑	PSNR↑	ESM↓	PSNR↑	LPIPS↓	ESM↓	PSNR↑	LPIPS↓
No Protect	1.0	0.00	NA	1.0	0.00	NA	1.0	NA	NA	1.0	NA	NA
Pretender	0.8691	0.01	30.08	0.8721	0.02	30.08	0.8164	30.09	0.1307	0.7393	30.09	0.1307
Adv-DM	0.8975	0.01	29.43	0.9092	0.01	29.43	0.8438	28.05	0.1488	0.7538	28.05	0.1488
ACE	0.9302	0.04	27.00	0.9346	0.02	27.00	0.7920	26.71	0.2042	0.7244	26.71	0.2042
CAAT	0.9561	0.05	32.08	0.9600	0.02	32.08	0.8467	32.55	0.1260	0.7326	32.55	0.1260
ours(specific)	0.0514	0.15	30.01	-0.011	0.16	30.26	0.0161	30.62	0.1109	0.2390	29.01	0.1505
ours(general)	0.1422	0.07	32.10	0.0685	0.19	32.10	0.1175	30.81	0.0980	0.2713	30.81	0.0980

anti-plagiarism, we choose IP-Adapter [24] and IP-Adapter-Plus [24], which utilize different layers of the embeddings encoded by CLIP [13].

For facial identity protection, Faceid uses the buffalo-pretrained model of ArcFace [2] and Instant-ID uses the antelopev2-pretrained model of ArcFace. The embedding dimensionality of ArcFace is 1×512 . For artwork anti-plagiarism, IP-Adapter uses the embedding encoded by CLIP, which is a 1×1024 tensors. IP-Adapter Plus uses the hidden state of CLIP [13], which is a 1280×768 . To save computing resources, we randomly sample b row vectors from the 1280 row vectors corresponding to one image for one iteration. In the experiments, b is set to 32 and 8 for the two tasks, respectively.

We train a pair of encryptor and decryptor for each image encoder. For the hyperparameter settings, we set the loss weights λ_1 to 1, λ_2 to 5, λ_3 to 1, λ_4 to 1, and λ_5 to 1. In Algorithm 1, the similarity threshold ths is set to 0.75 and 0.65 for two tasks, respectively. The budget ϵ is set to 11/255 and 21/255, respectively. All experiments are conducted on two NVIDIA 4090 GPUs.

4.2. Comparative Results

We compare Adapter Shield with four state-of-the-art open source methods: Pretender [20], Adv-DM [11], ACE [26], and CAAT [23]. These methods are tailored to protect images from being utilized to fine-tune diffusion models. For facial identity protection, we employ the identity cosine similarity (ISM) and abnormal face rate (such as occlusion and abnormal patterns in Figure 6) of generated images (AFR) as metrics. A lower ISM value combined with a higher AFR value indicates a more effective protection performance. For artwork anti-plagiarism, the embeddings cosine similarity (ESM) is utilized to assess the protection effectiveness. In addition, we exploit LPIPS [25] to evaluate the visual quality of protected images. For fair comparison, the PSNR of protected images across these methods are kept around 30. As shown in Table 1, our approach demon-



Figure 4. Visualization results of comparative experiments. “Reference” denotes the image prompt provided as input to FaceID/Instant-ID/IP-Adapter/IP-Adapter Plus. “No Protect” represents the original images without any protection.

strates universality across various zero-shot image-to-image generation methods and tasks, thereby safeguarding images against unauthorized generation. In contrast, existing methods are tailored to defend fine-tuning diffusion models, exhibiting limited generalization capacity to zero-shot methods. We present visualization results in Figure 4.

Table 2. Robustness evaluation under different distortions. The results denote the cosine similarity of embeddings between original images and distorted protected images. “Clean” represents protected images without distortions.

Type	Faceid	Ins-ID	IP-Ada	IP-Ada+
Clean	0.0514	-0.0110	0.0107	0.2523
Noise	0.1678	0.1742	0.1852	0.3864
Blur	0.1407	0.1285	0.0553	0.2890
JPEG	0.3682	0.3882	0.6870	0.6675

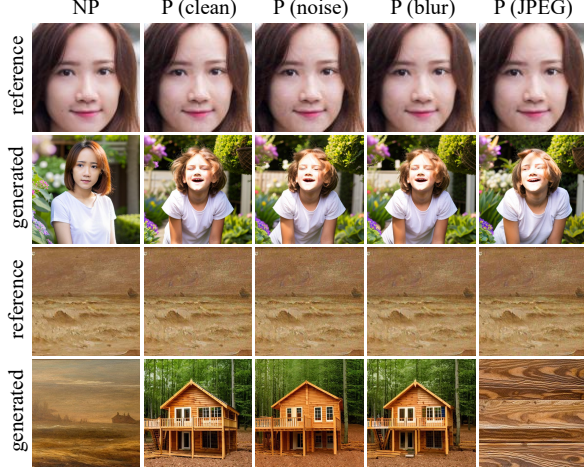


Figure 5. Robustness results of face identity protection and artwork anti-plagiarism.

4.3. Robustness Evaluation

This section evaluates the robustness against potential posting-processing operations applied by unauthorized users. We consider three categories of common image distortions that cannot impair generation quality: Gaussian noise, Gaussian blur, and JPEG compression. The mean and standard deviation of Gaussian noise are 0 and 0.01, respectively. The kernel size and standard deviation of Gaussian blur are 3×3 and 0.4. The quality factor of JPEG compression is 0.9. The above settings are justified by two key factors: (1) these operations are common image processing techniques that do not require the execution of complex programs and can be easily performed using smartphone or user-friendly software. (2) serious distortion may compromise the inherent content of images, resulting in outputs that are blurred or contain artifacts, which is undesirable for unauthorized users.

Table 3. Effects of encryption and decryption. Diversity is evaluated by computing the cosine similarity of embeddings encrypted or decrypted by different passwords. Lower similarity represents better diversity.

Model	Encrypt Effect↓	Decrypt Effect↑	Encrypt Diversity↓	Decrypt Diversity↓
Faceid	-0.0320	0.9927	0.0203	0.0434
Ins-ID	-0.0544	0.9725	0.0591	0.0966
IP-Ada.	-0.0244	0.9312	0.0509	0.1230
IP-Ada+	-0.0067	0.9217	0.1120	0.0612

The robustness results presented in Table 2 indicate that our protection solution is resilient enough to Gaussian noise and Gaussian blur because we augment the pipeline of Al-

gorithm 1 by adding differentiable image processing operations in iterations. For JPEG compression, the robustness of our approach is lower compared to the other two types of distortions, which suggests that the introduced adversarial perturbations are fragile to discrete cosine transform and quantization operations. We present some visualization results in Figure 5.

4.4. Performance of Encryption and Decryption

As the first authentication-integrated framework in this field, our approach can decrypt the encrypted embeddings to their original form with a correct password. As described in optimization objectives, the primary objective of the encryptor is to maximize the similarity between the encrypted embeddings and the original embeddings, whereas the decryptor aims to recover the encrypted embeddings that are as close as possible to the original ones. We evaluate the effectiveness of encryptor and decryptor through the cosine similarity between the encrypted/decrypted embeddings and the original embeddings. For diversity, we define encryption and decryption diversity as the cosine similarity between embeddings generated from the same input following encryption and decryption processes using different random passwords. Table 3 indicates that our approach achieves good performance on encryption effect, decryption effect, encryption diversity, and decryption diversity. We present visualization results in Figure 6.

4.5. Ablation Study

As shown in Table 4, the ablation experiments are divided into two parts. The diversity is defined as the cosine similarity of two embeddings.

Part 1: Encryption and Decryption. In this part, we evaluate the effect of \mathcal{L}_{div} and $\mathcal{L}_{div.s}$. The first sub-table in Table 4 demonstrates that \mathcal{L}_{div} can substantially enhance the diversity of the encrypted and decrypted results across various passwords. Furthermore, with the help of $\mathcal{L}_{div.s}$, the results conditioned on the same password can also exhibit substantial diversity as measured by “**Diversity Same pwd**”. We also evaluate the security of our approach by wrong decryption rate which represents the successful rate of decrypting with random passwords. Due to the balance requirement between diversity and encryption/decryption performance, the introduction of \mathcal{L}_{div} and $\mathcal{L}_{div.s}$ slightly increases the security risk of random password attack. The maximum wrong decryption rate remains as low as 5%, which has slight impact on the overall security of the proposed method. Visualization results are shown in Figure 7.

Part 2: the Impact of \mathcal{L}_{mt} . Finally, we conduct ablation experiments for \mathcal{L}_{mt} in Algorithm 1. In the third sub-Table of Table 4, “**w/o \mathcal{L}_{mt}** ” represents $m = 1$ in Eq. 9 and “**with \mathcal{L}_{mt}** ” represents $m = 2$ in Eq. 9. The metric “**Specific Similarity**” is the cosine similarity of embeddings extracted by

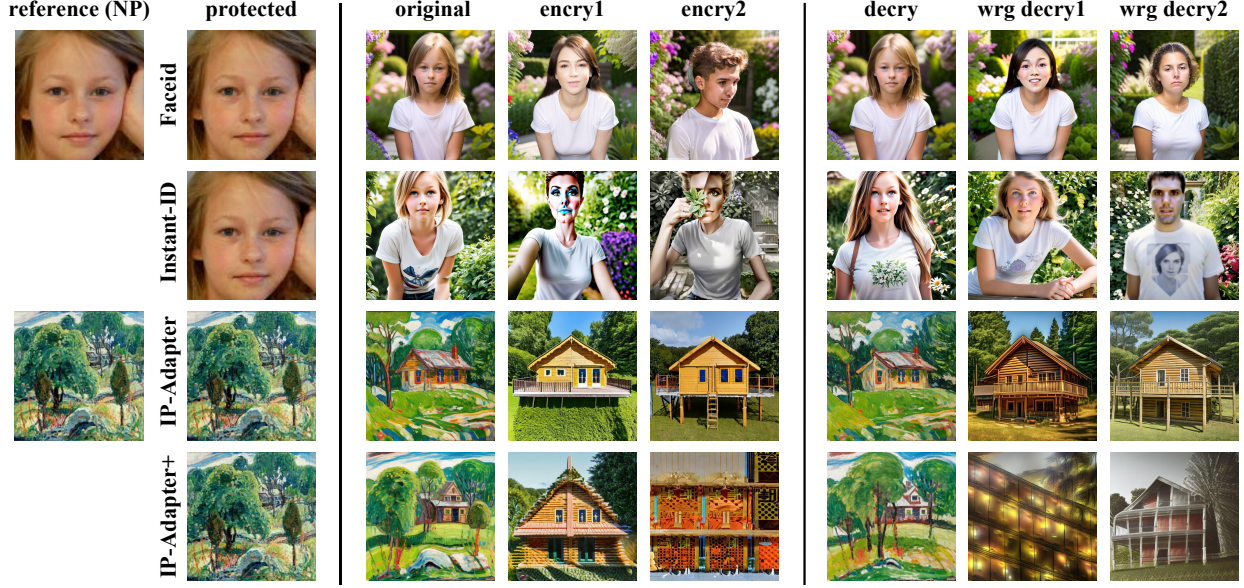


Figure 6. The visualization results of encryption and decryption performance. More visualization results are presented in supplementary materials. Text prompts: “*a young woman in white T-shirt in a garden*” and “*best quality, high quality, a wooden house in forest*”.

Table 4. Ablation study of different components. “Diversity Same pwd” represents the cosine similarity of embeddings encrypted by the same password for different images. “Wrong Dec Rate” represents the success rate of recovering original embeddings by random passwords. The cosine similarity threshold for successful recovery is set to 0.8.

Sub-Table	Model	Facial Identity Protection				Artwork Anti-Plagiarism			
		Encrypt Diversity↓	Decrypt Diversity↓	Diversity Same pwd↓	Wrong Dec Rate↓	Encrypt Diversity↓	Decrypt Diversity↓	Diversity Same pwd↓	Wrong Dec Rate↓
Part 1	w/o $\mathcal{L}_{div}, \mathcal{L}_{div.s}$	0.9849	0.9995	0.9993	0.0	0.4563	0.9927	0.9160	0.0
	w/o $\mathcal{L}_{div.s}$	-0.0137	0.0100	0.9958	0.0	0.0253	0.0159	0.9788	0.0
	with $\mathcal{L}_{div}, \mathcal{L}_{div.s}$	0.0232	0.0468	0.0361	0.015	0.082	0.086	0.5891	0.05
Part 2	Method	Specific Similarity↓	Unseen Similarity↓	PSNR↑	Time(s)↓	Specific Similarity↓	Unseen Similarity↓	PSNR↑	Time(s) ↓
	w/o \mathcal{L}_{mt}	0.02	0.2946	30.14	25.13	0.1276	0.5128	29.82	220.90
	with \mathcal{L}_{mt}	0.1054	0.1054	32.10	40.03	0.1944	0.1944	30.81	480.55

the utilized image encoder which is different in the case of “w/o \mathcal{L}_{mt} ”. The metric “Unseen Similarity” corresponds to the cosine similarity of embeddings extracted by other image encoders which is not considered in the case of “w/o \mathcal{L}_{mt} ”. The lower the values of these two metrics, the greater the distinction between the protected images and their original forms. These results demonstrate that \mathcal{L}_{mt} can enhance the generalization capacity of protected images against various zero-shot image-to-image generation methods.

5. Conclusion

This paper introduces Adapter Shield, the first universal and authentication-integrated framework designed to prevent unauthorized zero-shot image-to-image generation. Experiments show our method effectively defends against various zero-shot generation techniques across tasks, proving its broad applicability. It also allows authorized users to

recover original embeddings using password-based authentication. Future work will focus on improving robustness and visual quality.

6. Appendix

6.1. Supplementary Results

More Visualization Results of Robustness Evaluation: We present more visualization results of robustness evaluation in Figure 8.

More Visualization Results of Ablation Study: We present more visualization results of ablation study in Figure 9 and Figure 10. Due to space constraints in the main text, Figure 9 presents a high-resolution version of Figure 7 in the main text, along with a detailed caption for enhanced clarity and reference. In Figure 9, the results of the same item across different images are obtained by

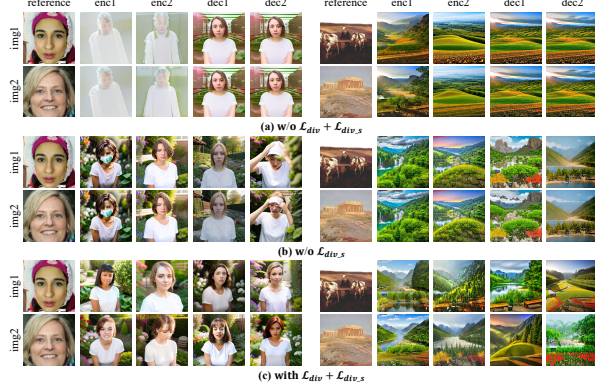


Figure 7. Visualization results of ablation results. The results of the same item across different images are obtained by the same passwords. More detailed captions are provided in our supplementary materials.

the same passwords. For instance, “enc1” across “img1” and “img2” are encrypted by the same passwords. “enc1” and “enc2” denote the encrypted results using two distinct passwords. “dec1” and “dec2” denote the decrypted results using two distinct and random passwords. As shown in Figure 9 (b), the loss function \mathcal{L}_{div} enhances the diversity of encrypted and decrypted results using different passwords (“enc1” vs “enc2”, “dec1” vs “dec2”). The loss function $\mathcal{L}_{div,s}$ improves the diversity of encrypted and decrypted results using the same password for different images (“enc1”/“enc2”/“dec1”/“dec2” across “img1” and “img2”). As shown in Figure 10, the loss function \mathcal{L}_{mt} enhances the universality across various zero-shot image-to-image generation methods.

More Visualization Results of Encryption and Decryption: We present more visualization results of encryption and decryption in Figure 11 and Figure 12.

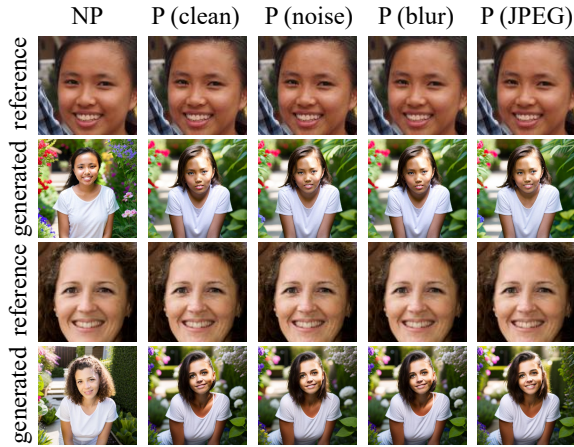


Figure 8. More visualization results of robustness evaluation. “NP” represents the original images without protection.

References

- [1] Jingyi Cao, Bo Liu, Yunqian Wen, Rong Xie, and Li Song. Personalized and invertible face de-identification by disentangled identity information manipulation. In *Proceedings of International Conference on Computer Vision*, pages 3314–3322, 2021. 4
- [2] Jiankang Deng, Jia Guo, Niannan Xue, and Stefanos Zafeiriou. Arcface: Additive angular margin loss for deep face recognition. In *Proceedings of the IEEE/CVF conference on computer vision and pattern recognition*, pages 4690–4699, 2019. 3, 5, 6
- [3] Rinon Gal, Yuval Alaluf, Yuval Atzmon, Or Patashnik, Amit H Bermano, Gal Chechik, and Daniel Cohen-Or. An image is worth one word: Personalizing text-to-image generation using textual inversion. *arXiv preprint arXiv:2208.01618*, 2022. 3
- [4] Xiuye Gu, Weixin Luo, Michael S Ryoo, and Yong Jae Lee. Password-conditioned anonymization and deanonymization with face identity transformers. In *European Conference on Computer Vision*, pages 727–743. Springer, 2020. 4
- [5] Zinan Guo, Yanze Wu, Chen Zhuowei, Peng Zhang, Qian He, et al. Pulid: Pure and lightning id customization via contrastive alignment. *Advances in Neural Information Processing Systems*, 37:36777–36804, 2024. 3
- [6] Edward J Hu, Yelong Shen, Phillip Wallis, Zeyuan Allen-Zhu, Yuanzhi Li, Shean Wang, Lu Wang, Weizhu Chen, et al. Lora: Low-rank adaptation of large language models. *ICLR*, 1(2):3, 2022. 3
- [7] Tero Karras, Samuli Laine, and Timo Aila. A style-based generator architecture for generative adversarial networks. In *Proceedings of the IEEE/CVF conference on Computer Vision and Pattern Recognition*, pages 4401–4410, 2019. 5
- [8] Nupur Kumari, Bingliang Zhang, Richard Zhang, Eli Shechtman, and Jun-Yan Zhu. Multi-concept customization of text-to-image diffusion. In *Proceedings of the IEEE/CVF Conference on Computer Vision and Pattern Recognition*, pages 1931–1941, 2023. 3
- [9] Dongze Li, Wei Wang, Kang Zhao, Jing Dong, and Tieniu Tan. RiDDLE: Reversible and Diversified De-identification with Latent Encryptor. In *Proceedings of the IEEE/CVF Conference on Computer Vision and Pattern Recognition*, pages 8093–8102, 2023. 4
- [10] Zhen Li, Mingdeng Cao, Xintao Wang, Zhongang Qi, Ming-Ming Cheng, and Ying Shan. Photomaker: Customizing realistic human photos via stacked id embedding. In *Proceedings of the IEEE/CVF conference on Computer Vision and Pattern Recognition*, pages 8640–8650, 2024. 3
- [11] Chumeng Liang, Xiaoyu Wu, Yang Hua, Jiaru Zhang, Yiming Xue, Tao Song, Zhengui Xue, Ruhui Ma, and Haibing Guan. Adversarial example does good: preventing painting imitation from diffusion models via adversarial examples. In *40th International Conference on Machine Learning, ICML 2023*, pages 20763–20786, 2023. 3, 6
- [12] Ziwei Liu, Ping Luo, Xiaogang Wang, and Xiaoou Tang. Deep learning face attributes in the wild. In *Proceedings of International Conference on Computer Vision*, pages 3730–3738, 2015. 5



Figure 9. More visualization results of ablation study on loss functions of encryption and decryption. The results of the same item across different images are obtained by the same passwords. For instance, “enc1” across “img1” and “img2” are encrypted by the same passwords. “enc1” and “enc2” denote the encrypted results using two distinct passwords. “dec1” and “dec2” denote the decrypted results using two distinct and random passwords.

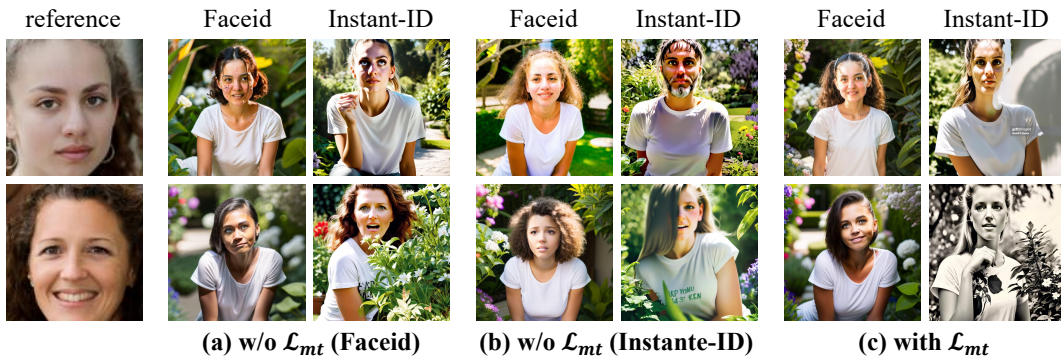


Figure 10. More visualization results of ablation study on multi-targeted loss function. (a) Minimizes cosine similarity only in the Faceid embedding domain. (b) Minimizes cosine similarity only in the Instant-ID embedding domain. (c) Minimizes cosine similarity in both Faceid and Instant-ID embedding domains.

[13] Alec Radford, Jong Wook Kim, Chris Hallacy, Aditya Ramesh, Gabriel Goh, Sandhini Agarwal, Girish Sastry, Amanda Askell, Pamela Mishkin, Jack Clark, et al. Learning transferable visual models from natural language supervision. In *International conference on machine learning*, pages

8748–8763. PmLR, 2021. 3, 6

[14] Robin Rombach, Andreas Blattmann, Dominik Lorenz, Patrick Esser, and Björn Ommer. High-resolution image synthesis with latent diffusion models. In *Proceedings of the IEEE/CVF Conference on Computer Vision and Pattern*



Figure 11. More visualization results of encryption and decryption performance. Text prompts: “*a young woman in white T-shirt in a garden*”.

- Recognition*, pages 10684–10695, 2022. 1
- [15] Nataniel Ruiz, Yuanzhen Li, Varun Jampani, Yael Pritch, Michael Rubinstein, and Kfir Aberman. Dreambooth: Fine tuning text-to-image diffusion models for subject-driven generation. In *Proceedings of the IEEE/CVF Conference on Computer Vision and Pattern Recognition*, pages 22500–22510, 2023. 3
- [16] Babak Saleh and Ahmed Elgammal. Large-scale classification of fine-art paintings: Learning the right metric on the right feature. *arXiv preprint arXiv:1505.00855*, 2015. 5
- [17] Shawn Shan, Jenna Cryan, Emily Wenger, Haitao Zheng, Rana Hanocka, and Ben Y Zhao. Glaze: Protecting artists from style mimicry by {Text-to-Image} models. In *32nd USENIX Security Symposium (USENIX Security 23)*, pages 2187–2204, 2023. 3
- [18] Shawn Shan, Wenxin Ding, Josephine Passananti, Stanley Wu, Haitao Zheng, and Ben Y Zhao. Nightshade: Prompt-specific poisoning attacks on text-to-image generative models. In *2024 IEEE Symposium on Security and Privacy (SP)*, pages 807–825. IEEE, 2024. 3

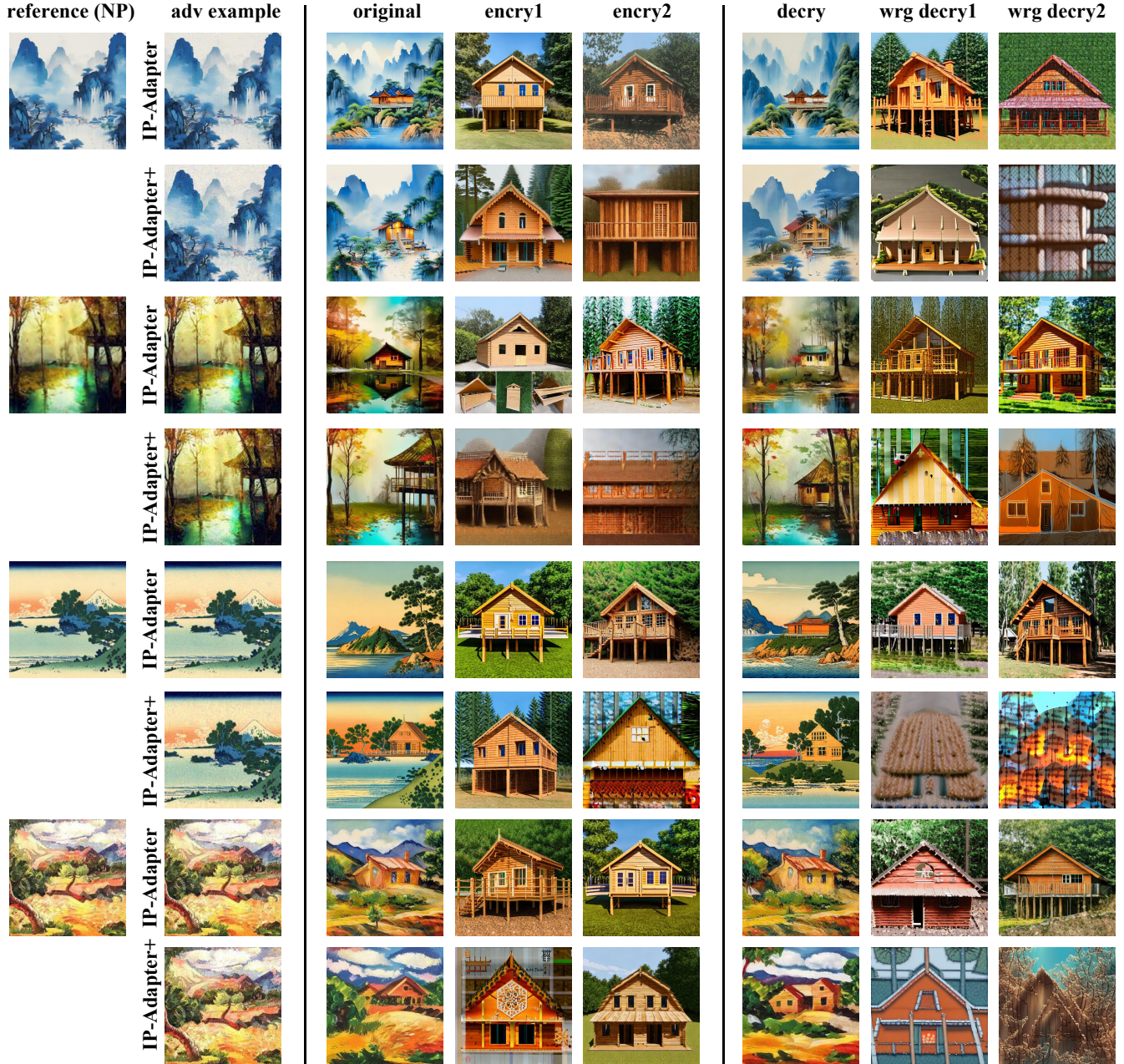


Figure 12. More visualization results of encryption and decryption performance. Text prompts: “*best quality, high quality, a wooden house in forest*”.

- [19] Yiren Song, Pei Yang, Hai Ci, and Mike Zheng Shou. Id-protector: An adversarial noise encoder to protect against id-preserving image generation. In *Proceedings of the IEEE/CVF conference on Computer Vision and Pattern Recognition*, pages 3019–3028, 2025. 2, 3
- [20] Zekun Sun, Zijian Liu, Shouling Ji, Chenhao Lin, and Na Ruan. Pretender: Universal active defense against diffusion finetuning attacks. In *The 34th USENIX Security Symposium*, 2025. 3, 6
- [21] Thanh Van Le, Hao Phung, Thuan Hoang Nguyen, Quan

- Dao, Ngoc N Tran, and Anh Tran. Anti-dreambooth: Protecting users from personalized text-to-image synthesis. In *Proceedings of International Conference on Computer Vision*, pages 2116–2127, 2023. 3
- [22] Qixun Wang, Xu Bai, Haofan Wang, Zekui Qin, and Anthony Chen. Instantid: Zero-shot identity-preserving generation in seconds. *arXiv preprint arXiv:2401.07519*, 2024. 3, 5
- [23] Jingyao Xu, Yuetong Lu, Yandong Li, Siyang Lu, Dongdong Wang, and Xiang Wei. Perturbing attention gives you more

- bang for the buck: Subtle imaging perturbations that efficiently fool customized diffusion models. In *Proceedings of the IEEE/CVF Conference on Computer Vision and Pattern Recognition*, pages 24534–24543, 2024. [3](#), [6](#)
- [24] Hu Ye, Jun Zhang, Sibor Liu, Xiao Han, and Wei Yang. Ip-adapter: Text compatible image prompt adapter for text-to-image diffusion models. *arXiv preprint arxiv:2308.06721*, 2023. [3](#), [5](#), [6](#)
- [25] Richard Zhang, Phillip Isola, Alexei A Efros, Eli Shechtman, and Oliver Wang. The unreasonable effectiveness of deep features as a perceptual metric. In *Proceedings of the IEEE/CVF conference on Computer Vision and Pattern Recognition*, pages 586–595, 2018. [6](#)
- [26] Boyang Zheng, Chumeng Liang, Xiaoyu Wu, and Yan Liu. Understanding and improving adversarial attacks on latent diffusion model. *openreview.net*, 2023. [3](#), [6](#)
- [27] Zhengguang Zhou, Jing Li, Huaxia Li, Nemo Chen, and Xu Tang. Storymaker: Towards holistic consistent characters in text-to-image generation. *arXiv preprint arXiv:2409.12576*, 2024. [3](#)